Received: 29 September 2022 | Revised: 9 January 2023 | Accepted: 6 February 2023

DOI: 10.1002/eco.2536

RESEARCH ARTICLE

WILEY

Hydrological dynamics and associated greenhouse gas fluxes in a mountain peatland under different climate scenarios

David J. Millar[1] | David J. Cooper[2] | Kathleen A. Dwire[3] | Robert M. Hubbard[3] | Michael J. Ronayne[4] | Joseph von Fischer[5]

[1]Pasture Systems and Watershed Management Research Unit, United States Department of Agriculture, Agricultural Research Service, East Wareham, Massachusetts, USA

[2]Department of Forest and Rangeland Stewardship, Colorado State University, Fort Collins, Colorado, USA

[3]USDA Forest Service Rocky Mountain Research Station, Fort Collins, Colorado, USA

[4]Department of Geosciences, Colorado State University, Fort Collins, Colorado, USA

[5]Department of Biology, Colorado State University, Fort Collins, Colorado, USA

Correspondence
David J. Millar, United States Department of Agriculture–Agricultural Research Service, Pasture Systems and Watershed Management Research Unit, One State Bog Rd., East Wareham, MA, USA.
Email: david.millar@usda.gov

Funding information
US Forest Service

Abstract

Peatlands have sequestered atmospheric carbon dioxide (CO_2) for millennia and can also act as significant sources of atmospheric methane (CH_4). Hydrological processes that control water table dynamics, and climatic conditions such as air temperature, play important roles in mediating peatland–atmosphere exchange of these greenhouse gases. These controls are likely to be impacted by climate change, particularly for those peatlands found in cold environments, including mountain regions. In this study, we developed empirical models to simulate hydrological dynamics and ecosystem–atmosphere C exchange in a mountain peatland under three climate scenarios (2012 air temperatures, +2°C and +4°C). Observed water table dynamics and air temperature were used to model ecosystem–atmosphere C exchange during the 2012 growing season. Modelled snowmelt dynamics were used to predict water table position at the beginning of the growing season for warming scenarios, and the subsequent water table dynamics and increased air temperature were used to drive the same C exchange models during the growing seasons. Increased air temperatures led to earlier snowmelt and water table decline, causing water tables to drop by 10 and 19 cm for the +2 and +4°C scenarios, respectively. This led to roughly a two-fold decrease in growing season net ecosystem production (NEP) in both warming scenarios, as a result of increased ecosystem respiration relative to gross primary production. Methane efflux was positively correlated with NEP and therefore decreased under the warming scenarios, albeit to a lesser degree. These results indicate that reductions in NEP and CH_4 efflux are possible in low-elevation mountain peatlands that are dependent on snowpack-derived hydrologic inputs. These ecosystems are found at elevations where future winter precipitation will increasingly fall as rain rather than snow and melting of snowpack will occur earlier under warmer conditions.

KEYWORDS
carbon dioxide, methane, mountain, peatland

1 | INTRODUCTION

Climate change is expected to have significant impacts on terrestrial ecosystem dynamics and hydrological cycles. Ecosystems characterized by cold climates, like those found in northern latitudes and mountain environments, are particularly susceptible to warmer temperatures, which can cause earlier melting of snow in the spring, potentially leading to decreased plant productivity due to drought stress later in the summer (Ernakovich et al., 2014; Parida & Buermann, 2014). In addition, warming of air to temperatures above freezing changes the phase of precipitation from snow to rain, potentially reducing annual snow accumulation, especially near elevations at the lower limit of snow persistence in the western United States (Ashfaq et al., 2013; Christensen & Lettenmaier, 2007), further altering the timing and magnitude of growing season hydrological fluxes (Godsey et al., 2014; Rood et al., 2008) and associated carbon (C) dynamics (Dong et al., 2019).

Of the ecosystems found in cold regions likely to be affected by a changing climate, peatlands are of particular concern, due to their dependence on a perennially high water table and their role in mediating fluxes of greenhouse gases (GHG) (Belyea, 2009). Water tables near the soil surface in northern peatlands favour the sequestration of carbon dioxide (CO_2), which has led to the accumulation of approximately one third of the terrestrial C on earth via organic soil formation (Gorham, 1991) and a net global cooling effect over the past 8000 to 11,000 years (Frolking & Roulet, 2007). However, a near-surface water table also creates an anoxic soil environment, which is responsible for peatlands being among the largest natural sources of atmospheric methane (CH_4) (Bridgham et al., 2013), a GHG with a global warming potential approximately 28 times greater than that of CO_2 at a century time scale (Myhre et al., 2013).

Climate change has the potential to alter peatland GHG dynamics indirectly by driving changes in hydrological cycles that affect water table position (WTP) (Moore et al., 1998). Water table manipulation experiments have shown that peatland ecosystem respiration (ER) increases when water tables decline (Chimner & Cooper, 2003a; Moore & Knowles, 1989; Riutta, Laine, & Tuittila, 2007). If water table declines in peatlands occur as a result of climate-driven changes in hydrological cycles, increases in ER can cause net ecosystem production (NEP) to decline, shifting these ecosystems from CO_2 sinks to sources (Riutta, Laine, Aurela, et al., 2007; Wu et al., 2013). Conversely, CH_4 emissions tend to decline with water table in peatlands, as greater proportions of the peat profile become exposed to oxic conditions (Gong et al., 2013; Turetsky et al., 2008). Further, peatland CH_4 emissions can be positively correlated with NEP (Bellisario et al., 1999; Whiting & Chanton, 1993) as methanogen substrate availability increases with NEP, as well as the potential for plant-mediated transport of CH_4, particularly in fens (Turetsky et al., 2014), all while maintaining the prerequisite anoxic soil environment. Future increases in air temperature (AT) also have the potential to impact GHG dynamics in peatlands directly, by increasing the metabolic rates of organisms that mediate fluxes of both CO_2 and CH_4 (Sullivan et al., 2007; Turetsky et al., 2008).

Peatlands similar to those in northern latitudes are found at high elevations in the Rocky Mountains of the western United States (Chimner et al., 2010) and have been sequestering atmospheric C for millennia (Chimner et al., 2002). The majority of precipitation falls as snow in the Rocky Mountains, and the snowpack typically persists through early summer at high elevations (Landry et al., 2014). While snowfall represents the majority of annual precipitation for this region, the San Juan Mountains of southwestern Colorado are also strongly influenced by the North American monsoon, with the highest monthly precipitation of the year occurring late in the summer (Costigan et al., 2000). In the San Juan Mountains, peatlands are found from approximately 2600 to 3700 m in elevation and contain plant species characteristic of peatlands in boreal regions of North America and Europe (Chimner et al., 2010). Because a warmer climate is likely to have the strongest influence on mountain snowpack at lower elevations (Christensen & Lettenmaier, 2007), it is likely that impacts on hydrological fluxes will be most pronounced to low-elevation peatlands (Millar et al., 2017). Such hydrological changes in low-elevation peatland found in the San Juan Mountains will potentially impact C budgets (Aurela, 2004) and extend the periods of water table decline between the onset of the snow-free season and the beginning of the monsoon season.

In this study, we used empirical models to simulate potential changes in hydrological dynamics and subsequently peatland–atmosphere C exchange at a low-elevation basin fen in the San Juan Mountains under warmer climate scenarios. The modelling effort included two phases. Changes in hydrological dynamics were first simulated as a function of AT to predict WTP under two warming scenarios. Then, using the observed and predicted water table dynamics along with increased AT under future climate scenarios, current and potential future growing season CO_2 and CH_4 fluxes were simulated.

2 | METHODS

2.1 | Study site

The study took place in a homogenous stand of *Carex lasiocarpa* at Anglica Fen (37°38′24″N, 107°47′45″W), an 8800-m^2 basin peatland surrounded by bedrock in the San Juan Mountains of southwestern Colorado at an elevation of approximately 2700 m. This site was chosen in part due to its location at the low end of the elevation range for peatlands in the region (Chimner et al., 2010) and therefore more susceptible to a changing climate (Millar et al., 2017). It was also chosen because of its comparatively simple water budget (Millar et al., 2018), due to lack of significant net groundwater flow (inflow–outflow), which would complicate the hydrological simulations under future climate scenarios presented here.

2.2 | Hydrological field measurements

Field observations were used to develop models of hydrological processes during the winter/spring and growing season of the 2012 snow year. An automated camera focused on a snow depth gauge, marked at 5-cm intervals, was installed at the site to track changes in snowpack and the duration of the snow-covered period at the site on a daily basis (Figure S1). Roughly once per week, snow depth observations measured at the site were compared with those at the Cascade #2 SNOTEL site, located approximately 1 km to the north at a very similar elevation (2747 m), and found to be highly correlated ($R^2 = 0.98$, slope = 1.0, $n = 17$). Therefore, daily precipitation and AT measured at the Cascade #2 SNOTEL site were used for winter/spring hydrological modelling.

An In-situ Barotroll and Rugged Troll (Fort Collins, CO) were installed at the site to measure AT, barometric pressure and WTP throughout the entire study period. A bias in WTP resulting from the influence of snowpack pressure was observed in which the water table increased 0.5 cm for every 1 cm of snow water equivalent (SWE) ($R^2 = 0.98$), so a regression of this bias was used to correct WTP during the snow-covered period. During the growing season, a Hobo Onset RG-2 was used to measure rainfall (Bourne, MA), and an Apogee Instruments SQ-110 quantum sensor (Logan, UT) was used to measure photosynthetically active radiation (PAR). All environmental variables were measured and logged hourly.

2.3 | GHG flux measurements

CO_2 and CH_4 efflux were measured roughly biweekly during the snow-free season of 2011 and monthly in 2012 using a dynamic closed soil chamber technique. Three ABS plastic collars, 60 cm × 60 cm, inserted approximately 5 cm into the soil, were used as the base for a 2.16×10^5 cm^3 cubic, clear gas flux chamber. Fluxes of CO_2, including NEP and ER, were measured in the field using a PP-Systems EGM-4 infrared CO_2 gas analyser. Shade cloth that reduced incoming PAR by 50% and 70% was used to capture NEP fluxes under a greater range of PAR values to improve model parameterization. In this study, positive NEP fluxes represent a net uptake of CO_2 by the ecosystem, while negative NEP fluxes represent a net loss of CO_2 to the atmosphere.

CH_4 efflux rates were determined using the chamber with a light-proof cover, collecting four midday gas samples at 10-min intervals, over 30 min. At each interval, 30 mL of chamber gas was sampled using a 50-mL syringe and transferred to a 20-mL evacuated vial. A Los Gatos methane/carbon dioxide/water vapour analyser (Mountain View, CA) was used to analyse CH_4 concentrations in each vial. A field blank composed of N_2 gas and a CH_4 standard (5.03 ppm) were used to ensure no changes in concentration occurred in CH_4 samples between field sampling and laboratory analysis. CH_4 flux rates were calculated as the slope of the linear regression between concentration and time (Turetsky et al., 2008), using only slope estimates where regression $R^2 \geq 0.95$.

2.4 | Modelling approach

The overall modelling effort was focused on two separate time periods: a hydrological model focused on the winter/spring (5 November 2011 to 5 March 2012) and a separate hydrological model combined with a biogeochemical model that estimated ecosystem CO_2 and CH_4 fluxes used during the growing season (1 June to 15 September 2012). Both the hydrological and biogeochemical models were run under three scenarios, using field data collected in 2011–2012, as well as two additional model runs, performed under potential future climate scenarios for the Rocky Mountains, in which hourly AT was increased by 2 and 4°C, respectively (Christensen & Lettenmaier, 2007; Liu et al., 2013).

2.5 | Winter/spring hydrological process modelling

The primary focus of the winter/spring hydrological model was to simulate changes in the phase of precipitation (rain or snow) along with snow accumulation and melting and their subsequent impact on water table dynamics preceding the growing season. Equation (1) represents the winter/spring WTP model.

$$\Delta WTP = rainfall + snowmelt - evaporation \tag{1}$$

Using mean daily AT, daily precipitation was partitioned into rain or snow using a sixth-order polynomial function, calibrated for the western United States, to calculate the probability of snow for ATs between 0.45 and 5.97°C (Auer, 1974). Within this temperature range, the mixed precipitation curve split total precipitation for a given time step into snow and/or rain (Fassnacht & Soulis, 2002). It was assumed that all precipitation fell as snow at daily mean ATs below 0.45°C and that all precipitation fell as rain above 5.97°C.

Once precipitation was partitioned into rain and snow, it was used to run a snowpack accumulation and melt model that predicted SWE on a daily time step, incorporating elements of a temperature-index snow model (TIM) (Bormann et al., 2014) that uses the snowmelt parameterization scheme of Rango and Martinec (1995). Daily melt potential was calculated using Equation (2).

$$Mp = MF\,(T_{mean} - T_{ref}) \tag{2}$$

In Equation (2), Mp represents snowmelt potential in cm day^{-1}, MF represents a melt parameter in cm °C^{-1} day^{-1}, T_{mean} represents daily mean AT in °C and T_{ref} represents the temperature above which melting occurs (set to 0°C in the study). Because MF varies depending on snow density, it was calculated on a daily basis using Equation (3).

$$MF = k\left(\frac{\rho_s}{\rho_w}\right) \tag{3}$$

In Equation (3), k is set to 1.1 cm °C^{-1} day^{-1}, according to Rango and Martinec (1995). Snow density in g cm^{-3} is represented by ρ_s, and ρ_w represents the density of water, which is set at 1 g cm^{-3}. As ρ_s varies throughout the snow-covered season, we used an on-site estimate of ρ_s along with a snow densification rate of 0.001 g cm^{-3} day^{-1} (Bormann et al., 2013) to estimate daily ρ_s throughout the snow-covered period. We used a federal sampler to conduct a snow survey near peak SWE for the water year at the site (14 March 2012) to estimate ρ_s ($\mu = 0.40$ g cm^{-3}, $\sigma = 0.033$ g cm^{-3}, $n = 13$). The mean ρ_s measured during the snow survey was used for 14 March, and daily ρ_s estimates for the remainder of the snow-covered season (before and after 14 March) were calculated using the snow densification rate.

Once developed, the precipitation and snowpack models were used to predict daily WTP during the winter/spring period, starting with an initial position of −3 cm (above the peat surface) observed on 4 November 2011. On each day, precipitation that fell as rain was available to recharge groundwater and raise the water table, while daily precipitation that fell as snow accumulated as snowpack. On days where *Mp* was >0, melt water was available for groundwater recharge in the same way as precipitation falling as rain, otherwise snow accumulated above the water table. Because WTP was above the soil surface (ponding) for the majority of winter/spring modelling period across scenarios, only briefly dropping ~2–3 below the peat surface in a few instances, readily available specific yield was not used to calculate changes in WTP.

The model was run using daily mean AT and precipitation data for the winter/spring period during the water year of 2012. Additional model runs were performed to simulate changes in winter/spring period WTP under two possible climate change scenarios for the Rocky Mountains, by increasing AT by 2 and 4°C (Christensen & Lettenmaier, 2007; Liu et al., 2013).

A snowpack persisted at the site throughout most of the 2011–2012 winter/spring modelling period. However, under the climate change scenarios, warmer ATs increase daily *Mp*, creating longer and more frequent snow-free periods, with WTPs above or just below the peat surface. Following snowmelt in 2012, we observed an above-ground water table that declined linearly at a rate of 0.4 cm day^{-1} from 6 April to 7 June ($R^2 = 0.97$), which spanned a range of mean daily ATs from −2.3 to 16.5°C. This daily decline in water table was interpreted as evaporation and incorporated into model runs for days with no snow cover, since no runoff or drainage was observed at the site during field visits while water was ponded above the soil surface following snowmelt.

2.6 | Growing season water table dynamics

From the 2012 growing season (1 June to 15 September), measured hourly WTPs were determined and used to model CO_2 dynamics during the growing season. For the warming scenarios, daily changes in WTP from 2012 were used; however, the initial WTP values at the beginning of the modelling period were adjusted based on pre-growing season conditions generated from the winter/spring hydrologic process modelling effort. This resulted in lower water tables throughout the growing season for both warming scenarios, as a result of earlier snowmelt and subsequent decline, relative to the 2012 observations. We set hourly changes in WTP under the warming scenarios to match that of the 2012 growing season based on an assumption that precipitation and evapotranspiration would have a similar effect on the position of the water table. Previous work at the site during the 2012 and 2013 growing season found that daily net groundwater fluxes at the site were minimal, suggesting that the water table at the site responds primarily to infiltrated precipitation and losses through evapotranspiration (Millar et al., 2018).

2.7 | Modelling ecosystem–atmosphere C exchange during the growing season

The CO_2 flux models applied to this study (gross primary production [GPP], ER and NEP) are described briefly here and in Millar et al. (2017). Chamber-based gas fluxes along with AT, PAR and WTP were used to empirically fit Bayesian models of ecosystem–atmosphere CO_2 exchange. Hourly GPP was modelled as a function of PAR and a running average of AT (RAV) as a proxy for phenology-based changes in photosynthetic biomass (Equation 4).

$$GPP_i = \frac{A_{max} \cdot \alpha \cdot PAR_i}{A_{max} + \alpha \cdot PAR_i} \cdot e^{\left[-0.5\left(\frac{RAV_i - RAV_{optGPP}}{RAV_{tolGPP}}\right)^2\right]} \tag{4}$$

In Equation (5), A_{max} (g CO_2 m^{-2} h^{-1}) represents the asymptotic maximum potential rate of GPP, and α (g CO_2 μmol PAR^{-1}) represents the light use efficiency, or initial slope of the light response function. The parameter RAV_{optGPP} (°C) represents the optimum value of RAV for GPP, and RAV_{tolGPP} (°C) represents the standard deviation of the Gaussian function, which controls the spread of the distribution.

Hourly ER was modelled as a function of WTP, AT and a RAV to also account for plant phenology and subsequent impacts on soil microbes (i.e., substrate availability). Because the warming scenarios used in this study resulted in water tables that were below those measured and used for model fitting, we modified the ER model of Millar et al. (2017) using an approach from Riutta, Laine and Tuittila (2007). In this way, we sought to better extrapolate beyond the data used to fit the model in a way that reflects the behaviour of peatland ER in response to declining water tables. For example, others have shown that peatland ER increases with water table decline down to a certain depth, beyond which changes in ER are diminished (Chimner et al., 2002; Riutta, Laine, & Tuittila, 2007).

$$ER_i = R_{10} \cdot Q_{10}^{\frac{AT_i - 10}{10}} \cdot \frac{1}{1 + e^{-1\left(\frac{WTP_i - b_1}{b_2}\right)}} \cdot e^{\left[-0.5\left(\frac{RAV_i - RAV_{optER}}{RAV_{tolER}}\right)^2\right]} \tag{5}$$

In Equation (5), R_{10} (g CO_2 m^{-2} h^{-1}) represents ER at an AT of 10°C when other model factors are not limiting, Q_{10} represents the rate of increase in ER per 10°C increase in AT, b_1 (cm) represents WTP at the steepest slope of ER change versus WTP and b_2 (cm^{-1}) represents the speed and direction of ER change versus WTP. RAV_{optER} (°C) and RAV_{tolER} (°C) represent the optimum RAV value for ER and the standard deviation of the Gaussian function controlling seasonality in ER, respectively.

Models were fit to measure data using Bayesian methods in R statistical software (R Development Core Team, Austria) using the *rjags* package (Plummer, 2011). A total of 100,000 iterations were used with four Markov chain Monte Carlo (MCMC) chains, after a burn-in of 20,000 iterations. Vague priors were used for all model parameters with the exception of b_1 and b_2 for the ER model presented here. For both of these parameters, uniform distributions ranging from −10 to 0 were used for prior distributions, to constrain the parameter space during MCMC based on realistic values for peatland ecosystems (Chimner et al., 2002; Riutta, Laine, Aurela, et al., 2007; Riutta, Laine, & Tuittila, 2007). Likelihood functions for both GPP and ER models were based on normal distributions, where $CO2_i^{obs}$ represents the observed flux, $\mu CO2_i$ represents the mean flux (g CO_2 m^{-2} h^{-1}) and $\sigma^2{}_{\text{proc }CO_2}$ represents the process variance (g CO_2 m^{-2} h^{-1}) associated with those predictions (Equation 6).

$$CO2_i^{obs} \sim Normal\left(\mu CO2_i, \sigma^2{}_{\text{proc }CO_2}\right) \tag{6}$$

WTP data collected in the growing season of 2012, as well as simulated WT position data for the +2 and +4°C climate change scenarios, were used as input data for the ER models for the three runs. Similarly, 2012 hourly AT was used for the 2012 growing season model run, while 2 and 4°C were added to each hourly measurement for the two climate change scenarios. Running averages of daily AT were also increased by 2 and 4°C for the GPP and ER models in their respective climate change scenarios.

A simple linear regression was used to model CH_4 efflux during the growing season as a function of NEP (Equation 7).

$$CH_{4i} = NEP_i \cdot \beta_0 + \beta_1 \tag{7}$$

In estimating model parameters, midday NEP and CH_4 fluxes at each collar location were used. As with the CO_2 flux models, the CH_4 model parameters were estimated using MCMC analysis in the *rjags* package for R (Plummer, 2011). Vague normal priors were used for all model parameters. Equation (8) represents the likelihood functions for the observed CH_4 ($CH4_i^{obs}$) as a function of NEP.

$$CH4_i^{obs} \sim Normal\left(\mu CH4_i, \sigma^2_{CH_4}\right) \tag{8}$$

In Equation (8), $\mu CH4_i$ represents the mean CH_4 flux (mg CH_4 m^{-2} h^{-1}) and $\sigma^2_{CH_4}$ represents the process variance (mg CH_4 m^{-2} h^{-1}) associated with those predictions. A total of 100,000 iterations were used with four MCMC chains, after a burn-in of 20,000 iterations, and the Gelman–Rubin diagnostic test was used to ensure convergence for all model parameters.

Growing season estimates of NEP, GPP, ER and CH_4 efflux were determined for all three scenarios, as the sum of hourly flux estimates. Entire posterior samples (n = 100,000 for each, propagating uncertainty from parameter estimates) for hourly CO_2 flux simulations were summed for NEP, GPP and ER using hourly environmental variables (e.g., AT, PAR and WTP). To calculate hourly CH_4 efflux, posterior mean estimates of simulated NEP were used as finite input values within the CH_4 model.

3 | RESULTS

3.1 | Snowpack and water table dynamics during the winter/spring period

Modelled daily SWE for the 2012 water year accurately captured changes in daily SWE observed at the Cascade #2 SNOTEL site (Figure 1). Additionally, modelled peak SWE (27 cm) on 4 March 2012 closely matched the measured peak SWE (26 cm) on 3 March 2012. Peak SWE under the +2°C scenario declined by almost half, to 15 cm (Table 1). Similarly, peak SWE under the +4°C scenario was almost half that of the +2°C scenario, at 8.0 cm. Snowmelt during the modelling period was progressively greater for the future climate scenarios. Six snow-free days occurred towards the end of the modelling period during the 2011–2012 winter/spring model run. Snow-free periods occurred more frequently and earlier in the winter/spring period during the modelling period for both climate change scenarios and persisted for longer, with 36 and 62 snow-free days for the +2 and +4°C scenarios, respectively (Figure 2).

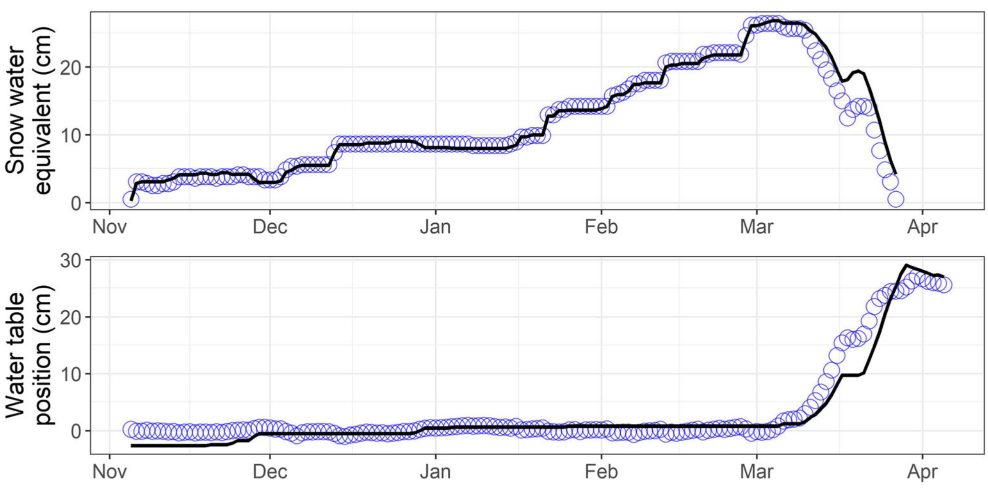

FIGURE 1 Observed versus simulated snow water equivalent and water table position from 5 November to 5 April during the 2012 snow year. Black lines represent simulated values and blue circles represent measured values. Positive values represent a water table above the soil surface, and negative values represent one below the soil surface.

TABLE 1 Modelled snow dynamics under three scenarios.

Scenario	Peak SWE (cm)	Mean SWE (cm)	Total snow-free period (day)	Number of snow-free periods
2012	27	11	6	2
+2°C	15	3.9	36	6
+4°C	8.0	1.6	62	11

Abbreviation: SWE, snow water equivalent.

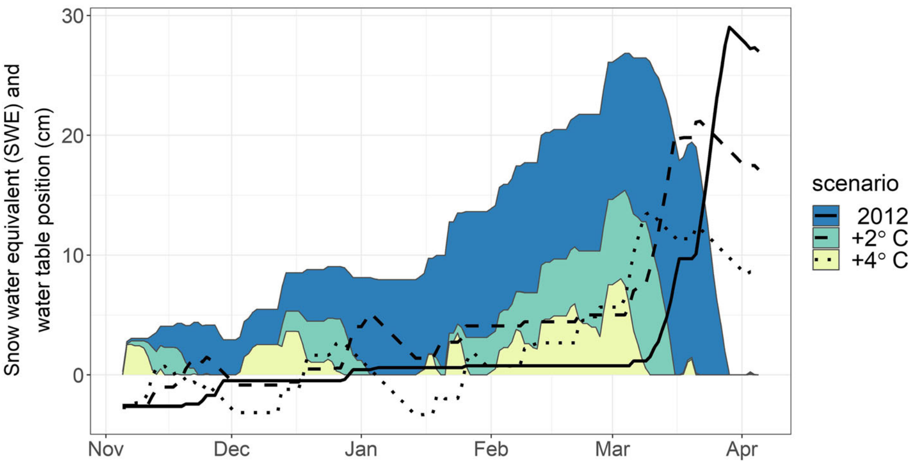

FIGURE 2 Snow water equivalent (SWE) and mean daily water table dynamics for all three modelling scenarios. Shaded areas represent SWE and heavy black lines represent water table position.

The modelled daily WTP closely followed ($R^2 = 0.94$) those that were observed through the winter/spring modelling period (Figure 1). Under the 2011–2012 model run, the water table remained stable during the winter/spring season, due to relatively little groundwater recharge derived from melting snow. Variations in the WTP were more frequent and of greater magnitude under the climate change scenarios; however, due to more frequent and substantial snowmelt events throughout the modelling period (Figure 2). Modelled water table on 5 April 2012 was within 1 cm of the observation for that date, at 27 cm above the peat surface in 2011–2012. Due to a greater frequency of snow-free days during the modelling period, both climate change scenarios had a greater evaporative loss from the water table, resulting in 5 April WTPs of 17 and 8 cm above the peat surface for the +2 and +4°C scenarios, which led to lower water tables during the growing season under these scenarios (Figure S2).

3.2 | Growing season environmental variables and ecosystem–atmosphere C exchange

Mean growing season ATs were 15.6, 17.6 and 19.6°C for the 2012, +2°C and +4°C scenarios (standard deviation = 6.5°C). Hourly AT showed strong daily oscillation, typical of the region, with a slight increasing daily trend towards the middle of the growing season followed by a slight decrease towards the end. Mean growing season WTP was −14, −24 and −33 cm for the 2012, +2°C and +4°C scenarios (standard deviation = 7.7 cm). For all scenarios, water tables generally followed a steady, general decline, with the exception of rapid, periodic increases resulting from monsoon-driven rain events occurring later in the growing season (Figure S2).

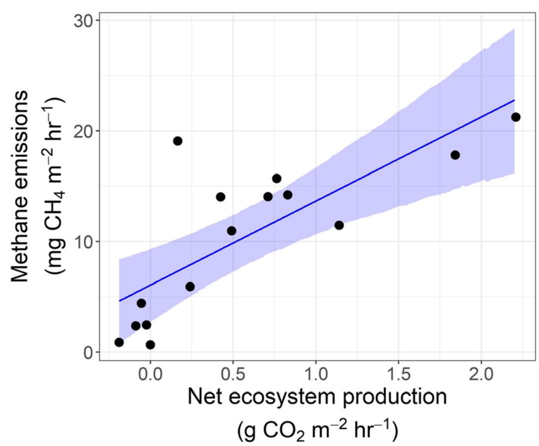

FIGURE 3 Observed midday CH_4 and NEP fluxes. Blue line represents the mean posterior prediction of the CH_4 linear regression model, with the shaded area representing the 95% highest density interval.

Observed GPP ranged from 0.03 to 3.01, and posterior mean model estimates matched observations reasonably well ($R^2 = 0.67$, $n = 78$) (Figure S3). Observed ER ranged from −0.01 to 1.06, and the ER model performed similarly to the GPP model ($R^2 = 0.66$, $n = 58$) (Figure S4). Measured NEP ranged from −0.20 to 2.21 g CO_2 m^{-2} h^{-1}, and measured CH_4 efflux ranged from 0.66 to 21 mg CH_4 m^{-2} h^{-1}. Midday measurements of CH4 efflux were positively correlated with midday measured NEP ($R^2 = 0.60$, $n = 15$) (Figure 3).

For all CO_2 and CH_4 flux model parameter estimates, uncertainty was quantified and varied among different parameters (Table 2 and

TABLE 2 Posterior parameter estimates for CO_2 and CH_4 flux models.

Gross primary production							
	Summary statistics		**Percentiles**				
Parameter	**Mean**	**Standard deviation**	**2.50%**	**25%**	**50%**	**75%**	**97.50%**
A_{max}	3.5	1.4	1.9	2.5	3.1	4.1	7.0
α	0.0034	0.0016	0.0015	0.0023	0.0030	0.0041	0.075
RAV_{opt}	22	4.1	16	19	22	26	30
RAV_{tol}	7.4	2.0	3.9	5.8	7.4	8.9	11
σ_{proc}	0.36	0.030	0.30	0.33	0.35	0.37	0.42
Ecosystem respiration							
	Summary statistics		**Percentiles**				
Parameter	**Mean**	**Standard deviation**	**2.50%**	**25%**	**50%**	**75%**	**97.50%**
Q_{10}	1.2	0.11	1.0	1.1	1.2	1.3	1.5
R_{10}	0.73	0.17	0.45	0.61	0.71	0.82	1.1
b_1	−0.69	0.69	−2.5	−0.95	−0.48	−0.20	−0.017
b_2	−8.7	1.3	−10.0	−9.6	−9.1	−8.3	−5.2
RAV_{opt}	21	4.9	14	16	20	25	29
RAV_{tol}	13	6.1	4.5	7.8	12	16	27
σ_{proc}	0.18	0.019	0.15	0.17	0.18	0.19	0.22
Methane efflux							
	Summary statistics		**Percentiles**				
Parameter	**Mean**	**Standard deviation**	**2.50%**	**25%**	**50%**	**75%**	**97.50%**
β_0	7.6	1.9	3.9	6.4	7.6	8.8	11
β_1	6.1	1.7	2.7	5.0	6.1	7.1	9.4
σ_{proc}	4.9	1.1	3.3	4.1	4.7	5.4	7.4

Figures S5 and S6). Modelled estimates of NEP during the 2012 growing season indicate that the site acted as a net source of CO_2 during 2012, with a mean flux rate of −310 g CO_2 m^{-2} gs^{-1}, while modelled mean CH_4 efflux for the same growing season was 13 g CH_4 m^{-2} gs^{-1}. Warming scenarios increased growing season fluxes of both GPP and ER, however, to a greater extent with ER, leading to an overall decreasing trend in NEP (Figure 4 and Table 3). The decrease in growing season NEP under the warming scenarios also drove a decrease in predicted CH_4 efflux, albeit to a lesser extent than CO_2 fluxes (Figure 5).

4 | DISCUSSION

4.1 | Water table dynamics under a future climate

The winter/spring period hydrological model simulated realistic changes in hydrological cycles under a warmer future climate. Future climate projections show that an increase in AT is expected for the Rocky Mountains (Christensen & Lettenmaier, 2007; Liu et al., 2013). However, climate models suggest that annual precipitation totals will remain highly variable from year to year, with no projected trend of increasing or decreasing precipitation (Harding et al., 2012). The hydrological simulations in this study present a plausible approach for identifying future changes in peatland hydrological cycles using changes in water table dynamics that could result from increased ATs in a mountainous environment (Christensen & Lettenmaier, 2007), for a given precipitation regime (that of 2011–2012 in this case). Worth noting, the warming scenarios presented here are simplistic representations of future climate conditions, simply increasing hourly temperatures observed in 2012. The results of this study should be considered in light of the fact that future increases in AT will likely be more stochastic.

Modelled daily changes in WTP closely followed observed changes, and only lagged observed rises slightly during the snowmelt period. Throughout the modelling period, the net flow of groundwater (inflow–outflow) was negligible, evident by the lack of increase or decrease in WTP during the 2012 winter/spring season, and also previous research conducted at the site (Millar et al., 2018). The +2 and +4°C climate change scenarios resulted in lower WTP throughout the growing season, 10–19 cm lower than levels measured in 2012. Similar projected water table declines, ranging from 14 to 22 cm under future climate conditions, have been projected for higher latitude fens in North America (Roulet et al., 1992).

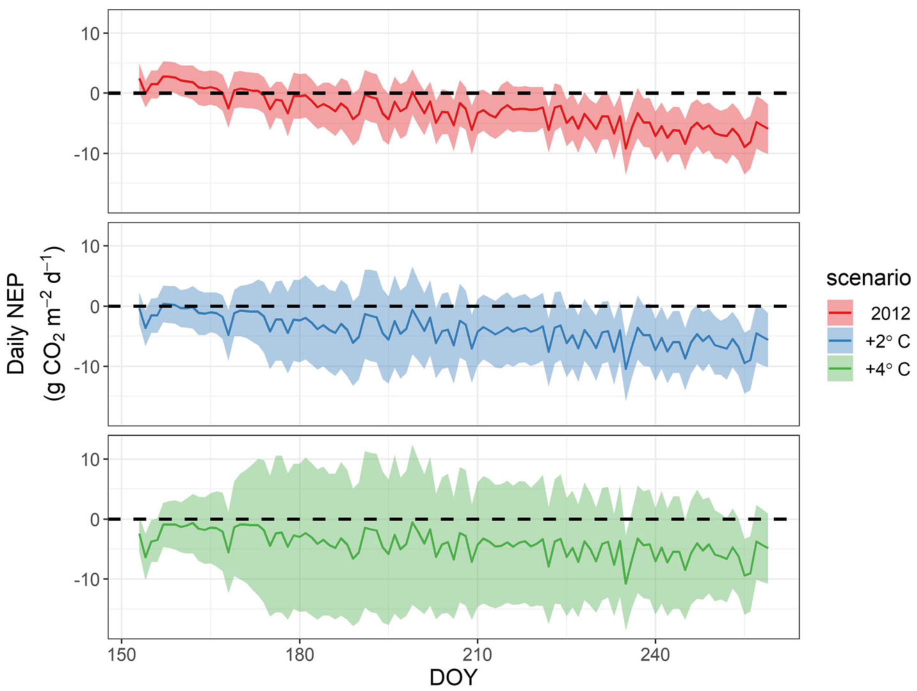

FIGURE 4 Simulated daily net ecosystem production (NEP) for three climate scenarios. Solid lines represent posterior mean NEP estimates and shaded areas represent the 95% highest density intervals. Values above the dashed horizontal lines represent net daily uptake of CO_2 while values below represent net losses to the atmosphere.

TABLE 3 Growing season gas exchange estimates for three scenarios.

		Posterior prediction	
Flux	Scenario	Mean	95% HDI
GPP (g CO_2 m^{-2} gs^{-1})	2012	1200	(1000, 1300)
	+2°C	1400	(1100, 1700)
	+4°C	1500	(870, 2100)
ER (g CO_2 m^{-2} gs^{-1})	2012	1500	(1100, 1800)
	+2°C	1800	(1400, 2300)
	+4°C	2000	(1200, 2700)
NEP (g CO_2 m^{-2} gs^{-1})	2012	−310	(−670, 65)
	+2°C	−420	(−970, 100)
	+4°C	−440	(−1400, 530)
CH_4 (g CH_4 m^{-2} gs^{-1})	2012	13	(3.8, 22)
	+2°C	12	(2.7, 22)
	+4°C	12	(2.5, 22)

Abbreviations: ER, ecosystem respiration; GPP, gross primary production; NEP, net ecosystem production; HDI, highest density interval.

In this study, the lower growing season water tables under the warming scenarios were primarily caused by earlier declines driven by increased loss of water via evaporation, lower peak SWE and longer periods of snow-free conditions during the winter and early spring. Similarly, declines in summer streamflow have been attributed to reductions in SWE over recent decades (Clow, 2010; Rood et al., 2008). Such declines are predicted to continue in mountainous regions of the western United States as more winter and spring precipitation falls as rain rather than snow (Godsey et al., 2014). Worth noting, sub-daily water table changes during future climate scenarios were calculated using the observed changes (i.e., the magnitude of change in response to a given amount of precipitation or evapotranspiration) during the 2012 growing season. In reality, a deeper water table may occur in peat with different hydraulic properties (e.g., lower specific yield), which could alter water table dynamics. Further, future changes in precipitation and/or evapotranspiration will also impact water table dynamics. These issues could be investigated further with a more highly parameterized hydrological modelling approach.

4.2 | Future ecosystem–atmosphere C exchange and implications for climate feedback

The measured and modelled fluxes of CO_2 and CH_4 in 2012 were similar to previously reported rates for peatlands in the Rocky Mountains (Chimner & Cooper, 2003b; Wickland et al., 2001). Modelled NEP was negative for the 2012 growing season at the study site; however, the CO_2 source/sink role for peatlands can vary from year to year as a result of inter-annual variability in environmental conditions (Fortuniak et al., 2021), including peatlands found in the Rocky Mountains (Millar et al., 2017). Peak SWE and summer precipitation were both below average at the site in 2012 (Millar et al., 2017), indicating that the low NEP for the growing season was due in part to drier conditions resulting in a lower water table. Increased ER under the warming scenarios, due to higher AT and lower water tables, resulted in further reductions of NEP, causing the site to function as a progressively stronger source of CO_2 to the atmosphere under warmer conditions. Similar reductions in peatland NEP resulting from increased ER under warmer future climate scenarios have also been projected for northern latitude peatlands (Chaudhary et al., 2022), many of which contain similar plant communities to those found in the Rocky

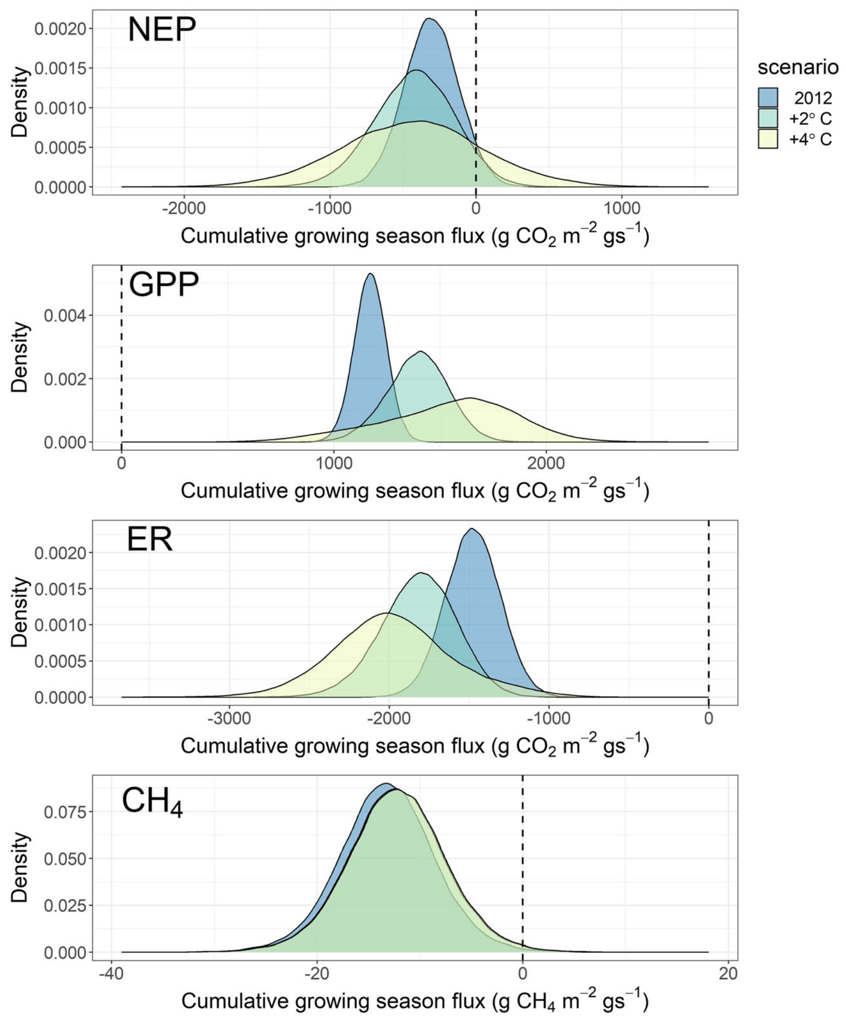

FIGURE 5 Posterior predictions of cumulative growing season flux estimates of methane emissions (CH_4), ecosystem respiration (ER), gross primary production (GPP) and net ecosystem production (NEP. Negative values presented here represent cumulative fluxes from the ecosystem to the atmosphere, and positive values represent cumulative fluxes from the atmosphere to the ecosystem.

Mountains. The site was a source of CH_4 under all three climate scenarios, and growing season efflux showed a slight decrease under the warming climate scenarios, resulting from lower NEP, which was driven by greater increases in ER relative to GPP.

The NEP model used in this study responded to AT and WTP in the same way. As AT increases, so does ER, and as the water table declines exposing more of the peat profile, it also causes ER to increase, driving decreases in NEP. Therefore, the important abiotic factors that control wetland CH_4 efflux are also incorporated in the NEP model used in this study. Although the CH_4 model used in this study was quite simplistic and only used NEP as a predictor variable, a correlation between CH_4 and NEP has been observed across a wide range of wetland types (Bellisario et al., 1999; Joabsson & Christensen, 2001; Whiting & Chanton, 1993). Increases in temperature drive increase CH_4 efflux rates, while declines in WTP can lead to decreased CH_4 efflux rates (Moore & Knowles, 1989; Turetsky et al., 2008, 2014). In this study, modelled NEP increased with WTP and AT, as CH_4 efflux tends to do in wetlands; higher temperatures increased biological activity and anoxic soil conditions promote methanogenesis.

An important consideration relating to growing season CH_4 fluxes estimated in this study is that CH_4 is transferred from peatland ecosystems to the atmosphere through three major pathways: diffusion through the soil, plant-mediated transport and ebullition events. Among these pathways, plant-mediated transport is often dominant, particularly for herbaceous, sedge-dominated peatlands (Bridgham et al., 2013). Given the strong correlation between CH_4 efflux and NEP observed in this study in a sedge-dominated plant community, modelled CH_4 presented is likely driven primarily by plant-mediated transport. Ebullition events, more stochastic in nature, were not considered in this study, although they can contribute significantly to overall CH_4 emission. Worth noting, what seemed as an 'outlier' point in Figure 4 (~20 mg CH_4 m^{-2} h^{-1}) could have potentially resulted from an ebullition event that occurred during the flux measurement and might explain why this flux was high relative to NEP, as compared with the other observations. Therefore, the CH_4 fluxes presented here potentially represent an underestimate of growing season totals, as they did not account for ebullition events, which can contribute from 18% to 50% of total CH_4 emissions in peatlands (Christensen et al., 2003).

Several sources of uncertainty exist for predicting future GHG fluxes. ER is estimated using Equation (5), which is driven in part by WTP. As mentioned above, future changes in water tables may not follow the exact dynamics presented here in the warming scenarios, which has implications for the responsiveness of ER dynamics, and ultimately NEP and CH_4, which were both indirectly driven by WTP in this study.

Plant community type plays an important role in controlling both CO_2 and CH_4 in wetland ecosystems (Johansson et al., 2006; Riutta, Laine, & Tuittila, 2007), and future changes in peatland plant community composition will likely result from warmer temperatures and lower water tables (McPartland et al., 2020; Munir et al., 2014; Weltzin et al., 2003). Such changes will likely have subsequent effects on ecosystem–atmosphere C exchange in these wetlands. Further, assuming that the present plant community dominated by *C. lasiocarpa* remains intact in the future, our approach does not consider any resilience (Yuan et al., 2017) or phenotypic plasticity (Li et al., 2016) that this vegetation may exhibit in response to changing climatic and environmental conditions, nor does it account for changes in NEP that may result from increases in growing season length (Gallego-Sala et al., 2018). Our approach assumed the plant community present during the time of field measurements would persist under a future climate and respond to future environmental conditions in a way consistent with observations in 2012 and 2013. Nevertheless, this study elucidates how ecosystem–atmosphere C exchange in a sedge-dominated peatland, an ecosystem type of great biogeochemical significance in boreal and mountain regions of the world (Belyea, 2009; Gorham, 1991; Turetsky et al., 2014), will potentially respond to a warming climate, providing conservative estimates of ecosystem–atmosphere C exchange under future climate scenarios. Further, the climate change scenarios in this study represent plausible changes in temperature and water table dynamics at peatlands similar to the study site.

Lastly, this study focuses on the fixed temporal window during the growing season (1 June through 15 September) in estimating ecosystem–atmosphere C exchange, representing less than a third of the year. Recent work in a mountain peatland similar to the one in this study, where NEP was measured continuously for three consecutive years, showed that the site only acted as a CO_2 sink during the same four-month period in all years. Others have also found that significant CO_2 losses, relative to annual fluxes, occur outside the growing season considered in this study (Nilsson et al., 2008). Therefore, it is likely that the net loss of CO_2 that occurred during the 2012 growing season in this study is likely a substantial underestimate of the CO_2 lost through ER over the course of the entire year.

5 | CONCLUSIONS

Our results show that simulated growing season GPP and ER for the study peatland increased under future warming scenarios. However, because ER increased disproportionately greater than that of ER, NEP ultimately decreased, causing the peatland to act as a strong CO_2 source under increasingly warmer conditions. The decrease was driven by lower water tables in the warming scenarios and also led to decreases in simulated CH_4 emissions. These ecosystem–atmosphere C exchange scenarios were all focused on the time of year with the greatest C sequestration potential. Uncertainty exists in our ability to predict future changes in ecosystem–atmosphere exchange of C in mountain peatlands. However, based on the results of this study, peatlands with similar hydroclimatic conditions and dependencies will potentially be at risk of accelerated rates of soil loss through decomposition under future climate conditions.

ACKNOWLEDGEMENTS

We thank the many students and field technicians whose contributions made this work possible. Funding for this study came from the United States Department of Agriculture, US Forest Service through the Rocky Mountain Research Station, in Fort Collins, Colorado.

DATA AVAILABILITY STATEMENT

The data that support the findings of this study are available from the corresponding author upon reasonable request.

REFERENCES

Ashfaq, M., Ghosh, S., Kao, S.-C., Bowling, L. C., Mote, P., Touma, D., Rauscher, S., & Diffenbaugh, N. S. (2013). Near-term acceleration of hydroclimatic change in the western U.S. *Journal of Geophysical Research-Atmospheres*, *118*(19), 10676–10693. https://doi.org/10.1002/jgrd.50816

Auer, A. H. (1974). The rain versus snow threshold temperatures. *Weatherwise*, *27*, 67. https://doi.org/10.1080/00431672.1974.9931684

Aurela, M. (2004). The timing of snow melt controls the annual CO_2 balance in a subarctic fen. *Geophysical Research Letters*, *31*(16), L16119. https://doi.org/10.1029/2004GL020315

Bellisario, L. M., Bubier, J. L., & Moore, T. R. (1999). Controls on CH 4 emissions from a northern peatland. *Global Biogeochemical Cycles*, *13*(1), 81–91.

Belyea, L. R. (2009). Nonlinear dynamics of peatlands and potential feedbacks on the climate system. In A. J. Baird, et al. (Eds.), *Carbon cycling in northern peatlands* (Vol. 184, pp. 5–18). Geophysical Monograph Series. AGU. https://doi.org/10.1029/2008GM000829

Bormann, K. J., Evans, J. P., & McCabe, M. F. (2014). Constraining snowmelt in a temperature-index model using simulated snow densities. *Journal of Hydrology*, *517*, 652–667. https://doi.org/10.1016/j.jhydrol.2014.05.073

Bormann, K. J., Westra, S., Evans, J. P., & McCabe, M. F. (2013). Spatial and temporal variability in seasonal snow density. *Journal of Hydrology*, *484*, 63–73. https://doi.org/10.1016/j.jhydrol.2013.01.032

Bridgham, S. D., Cadillo-Quiroz, H., Keller, J. K., & Zhuang, Q. (2013). Methane emissions from wetlands: Biogeochemical, microbial, and modeling perspectives from local to global scales. *Global Change Biology*, *19*(5), 1325–1346. https://doi.org/10.1111/gcb.12131

Chaudhary, N., Zhang, W., Lamba, S., & Westermann, S. (2022). Modeling pan-Arctic peatland carbon dynamics under alternative warming scenarios. *Geophysical Research Letters*, *49*(10), 1–9. https://doi.org/10.1029/2021GL095276

Chimner, R., Lemly, J. M., & Cooper, D. J. (2010). Mountain fen distribution, types and restoration priorities, San Juan Mountains, Colorado, USA. *Wetlands*, *30*(4), 763–771. https://doi.org/10.1007/s13157-010-0039-5

Chimner, R. A., & Cooper, D. J. (2003a). Influence of water table levels on CO2 emissions in a Colorado subalpine fen: An in situ microcosm study. *Soil Biology and Biochemistry*, *35*(3), 345–351. https://doi.org/10.1016/S0038-0717(02)00284-5

Chimner, R. A., & Cooper, D. J. (2003b). Carbon dynamics of pristine and hydrologically modified fens in the southern Rocky Mountains. *Canadian Journal of Botany*, *81*(5), 477–491. https://doi.org/10.1139/b03-043

Chimner, R. A., Cooper, D. J., & Parton, W. J. (2002). Modeling carbon accumulation in Rocky Mountain fens. *Wetlands (Wilmington)*, *22*(1), 100–110. https://doi.org/10.1672/0277-5212(2002)022[0100:MCAIRM]2.0.CO;2

Christensen, N. S., & Lettenmaier, D. P. (2007). A multimodel ensemble approach to assessment of climate change impacts on the hydrology and water resources of the Colorado River Basin. *Hydrology and Earth System Sciences*, *11*(4), 1417–1434. https://doi.org/10.5194/hess-11-1417-2007

Christensen, T. R., Panikov, N., Mastepanov, M., Joabsson, A., Öquist, M., Sommerkorn, M., Reynaud, S., Svensson, B., & Christensen, T. R. (2003). Biotic controls on CO_2 and CH_4 exchange in wetlands: A closed environment study. *Biogeochemistry*, *64*(3), 337–354. https://doi.org/10.1023/A:1024913730848

Clow, D. W. (2010). Changes in the timing of snowmelt and streamflow in Colorado: A response to recent warming. *Journal of Climate*, *23*(9), 2293–2306. https://doi.org/10.1175/2009JCLI2951.1

Costigan, K. R., Bossert, J. E., & Langley, D. L. (2000). Atmospheric/hydrologic models for the Rio Grande Basin: Simulations of precipitation variability. *Global and Planetary Change*, *25*, 83–110. https://doi.org/10.1016/S0921-8181(00)00023-0

Dong, Z., Driscoll, C. T., Campbell, J. L., Pourmokhtarian, A., Stoner, A. M. K., & Hayhoe, K. (2019). Projections of water, carbon, and nitrogen dynamics under future climate change in an alpine tundra ecosystem in the southern Rocky Mountains using a biogeochemical model. *Science of the Total Environment*, *650*, 1451–1464. https://doi.org/10.1016/j.scitotenv.2018.09.151

Ernakovich, J. G., Hopping, K., Berdanier, A. B., Simpson, R. T., Kachergis, E. J., Steltzer, H., & Wallenstein, M. D. (2014). Predicted responses of arctic and alpine ecosystems to altered seasonality under climate change. *Global Change Biology*, *20*, 3256–3269. https://doi.org/10.1111/gcb.12568

Fassnacht, S. R., & Soulis, E. D. (2002). Implications during transitional periods of improvements to the snow processes in the land surface scheme-hydrological model WATCLASS. *Atmosphere-Ocean*, *40*(4), 389–403. https://doi.org/10.3137/ao.400402

Fortuniak, K., Pawlak, W., Siedlecki, M., Chambers, S., & Bednorz, L. (2021). Temperate mire fluctuations from carbon sink to carbon source following changes in water table. *Science of the Total Environment*, *756*, 144071. https://doi.org/10.1016/j.scitotenv.2020.144071

Frolking, S., & Roulet, N. T. (2007). Holocene radiative forcing impact of northern peatland carbon accumulation and methane emissions. *Global Change Biology*, *13*(5), 1079–1088. https://doi.org/10.1111/j.1365-2486.2007.01339.x

Gallego-Sala, A., Charman, D. J., Brewer, S., Page, S. E., Prentice, I. C., Friedlingstein, P., Moreton, S., Amesbury, M. J., Beilman, D. W., Björck, S., Blyakharchuk, T., Bochicchio, C., Booth, R. K., Bunbury, J., Camill, P., Carless, D., Chimner, R. A., Clifford, M., Cressey, E., … Zhao, Y. (2018). Latitudinal limits to the predicted increase of the peatland carbon sink with warming. *Nature Climate Change*, *8*, 907–913. https://doi.org/10.1038/s41558-018-0271-1

Godsey, S. E., Kirchner, J. W., & Tague, C. L. (2014). Effects of changes in winter snowpacks on summer low flows: Case studies in the Sierra Nevada, California, USA. *Hydrological Processes*, *28*(19), 5048–5064. https://doi.org/10.1002/hyp.9943

Gong, J., Kellomäki, S., Wang, K., Zhang, C., Shurpali, N., & Martikainen, P. J. (2013). Modeling CO2 and CH4 flux changes in pristine peatlands of Finland under changing climate conditions. *Ecological Modelling*, *263*, 64–80. https://doi.org/10.1016/j.ecolmodel.2013.04.018

Gorham, E. (1991). Northern peatlands: Role in the carbon cycle and probable response to climatic warming. *Ecological Applications*, *1*(2), 182–195. https://doi.org/10.2307/1941811

Harding, B. L., Wood, A. W., & Prairie, J. R. (2012). The implications of climate change scenario selection for future streamflow projection in the Upper Colorado River Basin. *Hydrology and Earth System Sciences*, *16*, 3989–4007. https://doi.org/10.5194/hess-16-3989-2012

Joabsson, A., & Christensen, T. R. (2001). Methane emissions from wetlands and their relationship with vascular plants: An Arctic example. *Global Change Biology*, *7*, 919–932. https://doi.org/10.1046/j.1354-1013.2001.00044.x

Johansson, T., Malmer, N., Crill, P. M., Friborg, T., Akerman, J. H., Mastepanov, M., & Christensen, T. R. (2006). Decadal vegetation changes in a northern peatland, greenhouse gas fluxes and net radiative forcing. *Global Change Biology*, *12*(12), 2352–2369. https://doi.org/10.1111/j.1365-2486.2006.01267.x

Landry, C. C., Buck, K. A., Raleigh, M. S., & Clark, M. P. (2014). Mountain system monitoring at Senator Beck Basin, San Juan Mountains, Colorado: A new integrative data source to develop and evaluate models of snow and hydrologic processes. *Water Resources Research*, *50*(2), 1773–1788. https://doi.org/10.1002/2013WR013711.Received

Li, H., Yu, K., Ratajczak, Z., Nippert, J. B., Tondrob, D., Xu, D., Li, W., & Du, G. (2016). When variability outperforms the mean: Trait plasticity predicts plant cover and biomass in an alpine wetland. *Plant and Soil*, *407*(1–2), 401–415. https://doi.org/10.1007/s11104-016-2898-x

Liu, Y., Goodrick, S., & Stanturf, J. (2013). Future U.S. wildfire potential trends projected using a dynamically downscaled climate change scenario. *Forest Ecology and Management*, *294*, 120–135. https://doi.org/10.1016/j.foreco.2012.06.049

McPartland, M., Montgomery, R., Hanson, P., Phillips, J., Kolka, R., & Palik, B. (2020). Vascular plant species response to warming and elevated carbon dioxide in a boreal peatland. *Environmental Research Letters*, *15*, 124066. https://doi.org/10.1088/1748-9326/abc4fb

Millar, D. J., Cooper, D. J., Dwire, K. A., Hubbard, R. M., & von Fischer, J. (2017). Mountain peatlands range from CO_2 sinks at high elevations to sources at low elevations: Implications for a changing climate. *Ecosystems*, *20*(2), 416–432. https://doi.org/10.1007/s10021-016-0034-7

Millar, D. J., Cooper, D. J., & Ronayne, M. J. (2018). Groundwater dynamics in mountain peatlands with contrasting climate, vegetation, and hydrogeological setting. *Journal of Hydrology*, *561*(August 2017), 908–917. https://doi.org/10.1016/j.jhydrol.2018.04.050

Moore, T. R., & Knowles, R. (1989). The influence of water table levels on methane and carbon dioxide emissions from peatland soils. *Canadian Journal of Soil Science*, *69*, 33–38. https://doi.org/10.4141/cjss89-004

Moore, T. R., Roulet, N. T., & Waddington, J. M. (1998). Uncertainty in the effect of climatic change on the carbon cycling of Canadian peatlands. *Climate Change*, *40*, 229–245. https://doi.org/10.1023/A:1005408719297

Munir, T., Xu, B., Perkins, M., & Strack, M. (2014). Responses of carbon dioxide flux and plant biomass to water table drawdown in a treed peatland in Northern Alberta: A climate change perspective. *Biogeosciences*, *11*, 807–820. https://doi.org/10.5194/bg-11-807-2014

Myhre, G., Shindell, D., Bréon, F.-M., Collins, W., Fuglestvedt, J., Huang, J., Koch, D., Lamarque, J.-F., Lee, D., Mendoza, B., Nakajima, T., Robock, A., Stephens, G., Takemura, T., & Zhan, H. (2013). Anthropogenic and natural radiative forcing. In T. F. Stocker, D. Qin, G.-K. Plattner, et al. (Eds.), *Climate change 2013: The physical science basis. Contribution of working group I to the fifth assessment report of the intergovernmental panel on climate change*. Cambridge University Press.

Nilsson, M., Sagerfors, J., Buffam, I., Laudon, H., Eriksson, T., Grelle, A., Klemedtsson, L., Weslien, P., & Lindroth, A. (2008). Contemporary carbon accumulation in a boreal oligotrophic minerogenic mire—A significant sink after accounting for all C-fluxes. *Global Change Biology*, *14*(10), 2317–2332. https://doi.org/10.1111/j.1365-2486.2008.01654.x

Parida, B. R., & Buermann, W. (2014). Snow depth, density, and SWE estimates derived from GPS reflection data: Validation in the western US. *Geophysical Research Letters*, *41*(15), 5476–5483. https://doi.org/10.1002/2014GL060495

Plummer, M. (2011). Rjags: Bayesian graphical models using MCMC. http://CRAN.Rproject.org/package=rjags

Rango, A., & Martinec, J. (1995). Revisiting the degree-day method for snowmelt computations. *Journal of the American Water Resources Association*, *31*, 657–669. https://doi.org/10.1111/j.1752-1688.1995.tb03392.x

Riutta, T., Laine, J., Aurela, M., Rinne, J., Vesala, T., Laurila, T., Haapanala, S., Pihlatie, M., & Tuittila, E. S. (2007). Spatial variation in plant community functions regulates carbon gas dynamics in a boreal fen ecosystem. *Tellus B*, *59*(5), 838–852. https://doi.org/10.1111/j.1600-0889.2007.00302.x

Riutta, T., Laine, J., & Tuittila, E.-S. (2007). Sensitivity of CO_2 exchange of fen ecosystem components to water level variation. *Ecosystems*, *10*(5), 718–733. https://doi.org/10.1007/s10021-007-9046-7

Rood, S. B., Pan, J., Gill, K. M., Franks, C. G., Samuelson, G. M., & Shepherd, A. (2008). Declining summer flows of Rocky Mountain rivers: Changing seasonal hydrology and probable impacts on floodplain forests. *Journal of Hydrology*, *349*(3–4), 397–410. https://doi.org/10.1016/j.jhydrol.2007.11.012

Roulet, N. T., Moore, T. R., Bubier, J. L., & Lafleur, P. M. (1992). Northern fens: Methane and climate change. *Tellus B*, *44*, 100–105. https://doi.org/10.3402/tellusb.v44i2.15429

Sullivan, P. F., Arens, S. J. T., Chimner, R., & Welker, J. M. (2007). Temperature and microtopography interact to control carbon cycling in a high Arctic fen. *Ecosystems*, *11*(1), 61–76. https://doi.org/10.1007/s10021-007-9107-y

Turetsky, M. R., Kotowska, A., Bubier, J., Dise, N. B., Crill, P., Hornibrook, E. R. C., Minkkinen, K., Moore, T. R., Myers-Smith, I. H., Nykänen, H., Olefeldt, D., Rinne, J., Saarnio, S., Shurpali, N., Tuittila, E. S., Waddington, J. M., White, J. R., Wickland, K. P., & Wilmking, M. (2014). A synthesis of methane emissions from 71 northern, temperate, and subtropical wetlands. *Global Change Biology*, *20*(7), 2183–2197. https://doi.org/10.1111/gcb.12580

Turetsky, M. R., Treat, C. C., Waldrop, M. P., Waddington, J. M., Harden, J. W., & McGuire, A. D. (2008). Short-term response of methane fluxes and methanogen activity to water table and soil warming manipulations in an Alaskan peatland. *Journal of Geophysical Research*, *113*, G00A10. https://doi.org/10.1029/2007JG000496

Weltzin, J. F., Bridgham, S. D., Pastor, J., Chen, J., & Harth, C. (2003). Potential effects of warming and drying on peatland plant community composition. *Global Change Biology*, *9*, 141–151. https://doi.org/10.1046/j.1365-2486.2003.00571.x

Whiting, G. J., & Chanton, J. P. (1993). Primary production control of methane emission from wetlands. *Nature*, *364*, 794–795. https://doi.org/10.1038/364794a0

Wickland, K. P., Striegl, G., Mast, M. A., & Clow, D. W. (2001). Carbon gas exchange at a southern Rocky Mountain wetland, 1996-1998. *Global Biogeochemical Cycles*, *15*(2), 321–335. https://doi.org/10.1029/2000GB001325

Wu, J., Roulet, N. T., Sagerfors, J., & Nilsson, M. B. (2013). Simulation of six years of carbon fluxes for a sedge-dominated oligotrophic minerogenic peatland in Northern Sweden using the McGill Wetland Model (MWM). *Journal of Geophysical Research – Biogeosciences*, *118*(2), 795–807. https://doi.org/10.1002/jgrg.20045

Yuan, J., Wang, P., Weiner, J., Bian, H., Tang, Z., & Sheng, L. (2017). The effects of soil drying on the growth of a dominant peatland species, *Carex lasiocarpa*. *Wetlands*, *37*(6), 1135–1143. https://doi.org/10.1007/s13157-017-0946-9

SUPPORTING INFORMATION

Additional supporting information can be found online in the Supporting Information section at the end of this article.

How to cite this article: Millar, D. J., Cooper, D. J., Dwire, K. A., Hubbard, R. M., Ronayne, M. J., & von Fischer, J. (2023). Hydrological dynamics and associated greenhouse gas fluxes in a mountain peatland under different climate scenarios. *Ecohydrology*, e2536. https://doi.org/10.1002/eco.2536